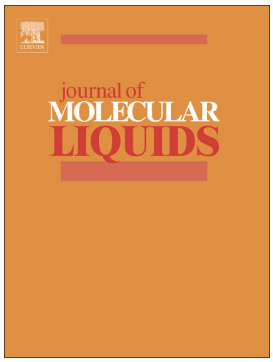

Effect of the surface functionalization of a waste-derived activated carbon on pharmaceuticals' adsorption from water

Guilaine Jaria, Mirtha A.O. Lourenço, Carla Patrícia Silva, Paula Ferreira, Marta Otero, Vânia Calisto, Valdemar I. Esteves

PII: S0167-7322(19)34972-4

DOI: https://doi.org/10.1016/j.molliq.2019.112098

Reference: MOLLIQ 112098

To appear in: *Journal of Molecular Liquids*

Received date: 9 September 2019

Revised date: 7 November 2019

Accepted date: 8 November 2019

Please cite this article as: G. Jaria, M.A.O. Lourenço, C.P. Silva, et al., Effect of the surface functionalization of a waste-derived activated carbon on pharmaceuticals' adsorption from water, *Journal of Molecular Liquids*(2019), https://doi.org/10.1016/j.molliq.2019.112098

Effect of the surface functionalization of a waste-derived activated carbon on pharmaceuticals' adsorption from water

Guilaine Jaria[a], *Mirtha A.O. Lourenço*[b,c], *Carla Patrícia Silva*[a], *Paula Ferreira*[b], *Marta Otero*[d], *Vânia Calisto*[a*], *Valdemar I. Esteves*[a]

[a] CESAM & Department of Chemistry, University of Aveiro, Campus Universitário de Santiago, 3810-193 Aveiro, Portugal

[b] CICECO & Department of Materials and Ceramic Engineering, University of Aveiro, Campus Universitário de Santiago, 3810-193 Aveiro, Portugal

[c] Istituto Italiano di Tecnologia, Center for Sustainable Future Technologies, Via Livorno, 60, 10144 Torino, Italy

[d] CESAM & Department of Environment and Planning, Campus Universitário de Santiago, 3810-193 Aveiro, Portugal

*Corresponding author. E-mail: vania.calisto@ua.pt (Vânia Calisto)

Telf.: (+351) 234 370 200

Abstract

The functionalization of a paper mill sludge-based activated carbon (AC) was addressed in this work for the first time. Four different procedures have been accomplished in order to introduce amine functional groups (AC-NH_2 and AC-APTES), thiol functional groups (AC-MPTMS), and a covalent organic polymer (AC-COP) onto the AC surface. The materials were characterized showing that the functionalization was succeeded, with a reduction of the specific surface area (S_{BET}), except for AC-MPTMS. The produced ACs were tested for the removal of six pharmaceuticals - carbamazepine (CBZ), lorazepam (LOR), sulfamethoxazole (SMX), piroxicam (PIR), paroxetine (PAR), and venlafaxine (VEN) - from different matrices (ultrapure water, ultrapure water with pH adjusted to 7.6, and effluent from a municipal wastewater treatment plant (WWTP)). The results indicated textural parameters, S_{BET}, micropore area and micropore volume, as the main factors influencing the adsorption, except for AC-NH_2 which showed a great specificity for PAR and VEN. Also, AC-MPTMS presented a high removal percentage of the antibiotic SMX in wastewater. Overall, AC-MPTMS and AC-APTES provided, respectively, the best and the poorest adsorptive performance. Although the functionalization did not result in the enhancement of pharmaceuticals' adsorption as compared with the parent AC, the selectivity for some pharmaceuticals was highly improved.

Keywords: Amination, Organosilane grafting, Adsorption, Wastewater treatment, Emerging contaminants

1. Introduction

Pharmaceuticals are a group of chemical substances, considered as emerging contaminants, which continuously enter the environment. The presence of these compounds in aquatic systems is well documented [1–4] and different sources were pointed out as the most relevant pathways of these compounds into the environment, mostly, urban, industrial or hospital wastewater treatment plants (WWTP), and aquaculture facilities [2]. Since pharmaceuticals were designed to induce a physiological response, their presence in the aquatic environment is concerning because of their potential to affect aquatic and human life [2,5]. European Union (EU) has already taken some preventive measures involving the monitoring of priority substances, where some pharmaceuticals were already included [6] assuming the need to develop effective strategies for water remediation.

Among the different treatments for the removal of pharmaceuticals from water, adsorptive processes stand out for being efficient and easy to implement and avoiding the generation of transformation products [7]. Although commercially available activated carbon (AC) has been extensively studied for such application, the adsorptive removal of pharmaceuticals using alternative materials is a subject that has been addressed by several authors [8–10]. In this context, paper mill sludge-based AC has been recently reported to have a comparable or even higher performance than commercial AC for adsorption of pharmaceuticals from water [11]. Furthermore, in line with the circular economy paradigm, the production of such an AC means an environmental and economical sustainable management route for the waste produced in huge amounts by the paper industry.

AC are characterized by a large specific surface areas (S_{BET}) providing high adsorption capacity per mass unit. However, AC lack selectivity towards pharmaceuticals, which would be a relevant feature for the removal of these contaminants since their

concentration in wastewater is quite low as compared with others. Still, since pharmaceuticals from a vast number of therapeutic classes and with very different properties have already been identified in wastewater and environmental compartments [11,12], it would be also desirable to have an AC presenting high efficiency towards distinct pharmaceuticals. Therefore, apart from high S_{BET}, chemical surface features for interaction with the target pharmaceuticals could be beneficial for increasing the efficiency of AC in drug adsorption-separation.

In general, the modification of the AC surface has been mainly addressed in terms of oxidation, acidic or basic treatments [13–16]. The resulting materials, applied to water treatment, have been used for the removal of metal ions, or organic pollutants such as dyes, phenols, naphthalenesulphonic acids, dibenzothiophene, benazolin, 2,4-dichlorophenoxy acetic acid, and atrazine [16]. There are few examples concerning the application for the removal of pharmaceuticals from water, as the work by Guedidi *et al*. [12], who studied the adsorption of ibuprofen onto AC cloths modified by NaOCl oxidation and thermal treatment under nitrogen atmosphere, and that by Bhadra *et al*. [17], who carried out an AC modification by oxidation with further application in the adsorption of diclofenac. Also, some biologically modified AC were tested for the removal of organic contaminants, such as methyl tert-butyl ether, natural organic matter and organic micropollutants (17β-estradiol, pesticides and bromate) [16]. Mines *et al*. [18], who highlighted the relevance of AC functionalization to expand their application for a wider range of pollutants, grafted a covalent organic polymer (COP) on the surface of an AC and tested the functionalized material in the removal of an azo dye and cadmium from water, resulting in a significant increase in the adsorption of the first. Besides these examples, the functionalization of AC

has been mostly studied for catalytic applications [19,20] and carbon electrodes [21,22], to get some insights on reaction mechanisms [23,24].

In this context, the main aim of this work was to evaluate the effects of different chemical functionalization methodologies on the properties of a paper mill sludge-based AC for application in the removal of pharmaceuticals from water. For this purpose, the referred AC was modified recurring to four different functionalization methods, namely: direct amination to enhance the percentage of amine functional group [25], organosilane grafting with (3-aminopropil)triethoxysilane (APTES, with impact on the nitrogen content), organosilane grafting with (3-mercaptopropyl)trimethoxysilane (MPTMS, influencing the sulfur content) [26], and functionalization with a covalent organic polymer (COP) [18]. After a full characterization of the produced materials, they were tested for the adsorption of 6 pharmaceuticals from different classes and with different physicochemical properties in order to assess the impact of functionalization and allowing to select the most promissory modification route(s) for the target application.

2. Experimental

2.1. Chemicals and reagents

The AC chemical functionalization was achieved using the following reagents: ethanol (99.9%, Riedel-de Haën), hydrochloric acid (HCl, 37% *v/v*, Carlo Erba), sulfuric acid (H_2SO_4, 95-97% *v/v*, PanReac), tin chloride ($SnCl_2$, 98%, Sigma-Aldrich), isopropylamine (99.5%, Aldrich), (3-mercaptopropyl)trimethoxysilane (MPTMS, 95%, Aldrich), (3-aminopropyl)triethoxysilane (APTES, 95%, Aldrich), toluene (99.8%, Aldrich), dichloromethane (CH_2Cl_2, 99.9%, Sigma-Aldrich), thionyl chloride ($SOCl_2$, 99%, Fluka), melamine ($C_3H_6N_6$, 99%, Aldrich), dimethyl sulfoxide (DMSO, ≥99.5%, Sigma-

Aldrich), diisopropylethylamine (DIPEA, 99%, Aldrich), terephthalaldehyde (>98.0%, TCI). The pharmaceuticals used for the adsorption experiments were carbamazepine (CBZ, Sigma-Aldrich, 99%), sulfamethoxazole (SMX, TCI, >98%), paroxetine (paroxetine-hydrochloride, PAR, TCI, >98%), lorazepam (LOR, Sigma-Aldrich, 99%), piroxicam (PIR, Sigma-Aldrich, 99%) and venlafaxine (VEN, TCI, >98%).

2.2. Materials synthesis

2.2.1. AC synthesis

The AC synthesis was performed as described by Jaria et al. [11]. Briefly, primary paper mill sludge (PS) was impregnated with a chemical activating agent (potassium hydroxide at a *w*:*w* ratio of 1:1). The impregnated PS was sonicated during 1 h in an ultrasound bath, dried at room temperature and then in an oven overnight at 105 °C. Subsequently, the material was subjected to pyrolysis under inert atmosphere, at 800 °C and for 150 min. The obtained carbon was then washed with hydrochloric acid (1.2 M), for the removal of ashes, and distilled water until the washing leachate reached neutral pH. The resulting material was oven dried at 105 °C and stored in a sealed container.

2.2.2. Functionalization of AC

The material from the previous step was used as precursor for the production of 4 different functionalized AC: AC-NH_2, AC-APTES, AC-MPTMS and AC-COP. The procedures for obtaining these functionalized AC are described next and summarized in Figure 1.

Direct amination

In order to yield AC-NH_2, the introduction of the amine functionalities into the phenylene moieties of the produced AC was reached using a two-step procedure described by Inagaki *et al*. for periodic mesoporous organosilica (PMO) [27] materials [25,28]. In a typical synthesis, the phenylene groups of AC (0.125 g) were first nitrated using concentrated acid solutions of HNO_3 (0.7 mL) and H_2SO_4 (2.2 mL). After stirring at room temperature during 72 h, the obtained AC-NO_2 was filtered-off, washed with distilled water and dried at 60 °C. Then, the AC-NO_2 (0.102 g) was treated with $SnCl_2$ (0.338 g) and HCl (3.2 mL) solution in order to reduce the nitro group to amine functionalities. The mixture was stirred at room temperature during 72 h. The obtained AC-NH_2 was filtered-off, washed with distilled water followed by isopropylamine-ethanol solution, and finally it was dried overnight at 60 °C (Figure 1A).

Organosilane grafting

The AC-APTES and AC-MPTMS materials were obtained from AC using a similar procedure used to functionalize PMO materials [26]. After the activation of the pores of the AC material (0.125 g), dry toluene (5 mL) was added. Then APTES (0.192 mL) or MPTMS (0.154 mL) were added drop wise to the suspension to obtain AC-APTES and AC-MPTMS, respectively. The mixtures were vigorously stirred for 24 h. The functionalized AC were filtered off, washed with dry toluene to remove unreacted species and further washed with a large amount of distilled water. Finally, both materials were dried overnight in an oven at 60 °C (Figure 1 B and C).

Functionalization with an organic polymer

The covalent organic polymer attached AC (AC-COP) was synthetized using a procedure similar to that reported by Mines *et al.* [18]. First, the oxidation of the AC (resulting in AC-Ox) was made by refluxing 5 g of AC with 50 mL of concentrated HNO_3 during 24 h. The AC-Ox was further washed with large amount of ultrapure water until reaching neutral pH. Then the AC-Ox was oven dried at 110 °C for 72 h. After activation of AC-Ox in vacuum at 110 °C, 1 g of this material was refluxed under nitrogen atmosphere with a mixture of 40 mL CH_2Cl_2, and 20 mL $SOCl_2$. After 24 h, the acylchloride modified AC (AC-Thio) was obtained by removing the solvent by vacuum distillation. Finally, a melamine modified AC material (AC-Mel) was obtained as follows: under inert conditions, 2 g of AC-Thio were treated with a sonicated solution of 0.150 g of melamine dissolved in 60 mL of DMSO and 1 mL of DIPEA. The mixture was heated to 120 °C for 24 h. The AC-Mel material was filtered, washed three times each with DMSO, ultrapure water and ethanol and dried in vacuum for 8 h at 110 °C. The preparation of AC-COP was made in a typical synthesis, where 0.368 g of melamine and 0.23 g of terephthalaldehyde were sonicated with 69 mL of DMSO under N_2 atmosphere. Then, 0.460 g of AC-Mel material were added into the solution, under inert atmosphere. The obtained mixture was stirred under reflux for 48 h. The AC-COP material was filtered-off, further washed three times with DMSO, acetone, ultrapure water and ethanol and finally, it was dried (Figure 1D).

2.3. Characterization of the synthesized materials

The AC and functionalized AC were characterized by -196 °C N_2-sorption isotherms, elemental analysis (EA), Attenuated Total Reflectance Fourier transformed infrared (ATR-FTIR) spectroscopy, Raman spectroscopy, thermogravimetric analysis

(TGA), and point of zero charge (pH_{pzc}). Also, AC-NH_2 and AC-MPTMS, which were the functionalized AC presenting the best results in terms of adsorption percentage, were further analyzed by X-Ray photoelectron spectroscopy (XPS) and scanning electron microscopy (SEM). More information concerning the used characterization techniques (specific methods, equipment models and conditions used) can be found in the electronic supplementary information (ESI).

2.4. Adsorptive removal of pharmaceuticals from water

Batch adsorption experiments were performed to evaluate the efficiency of the AC and functionalized AC for the removal of six different pharmaceuticals from water: the anti-epileptic CBZ, the anxiolytic LOR, the antibiotic SMX, the non-steroidal anti-inflammatory PIR, and the antidepressants PAR and VEN. These six compounds were chosen for this study so to encompass pharmaceuticals from different therapeutic classes, with different pK_a, and different chemical structures (please see Table S1 in ESI for more details). This selection aimed at finding out possible connections between adsorption behavior, pharmaceuticals properties and the features of the AC.

Single component pharmaceutical solutions, with an initial concentration of 5 $mg \cdot L^{-1}$, were prepared and put in contact with each produced material (at a dosage of 25 $mg \cdot L^{-1}$) in 50 mL polypropylene tubes. This dose of material, based on preliminary studies, was selected in order to have quantifiable removal percentages of each pharmaceutical under the studied conditions. In this way, it was avoided using different doses for different systems, which would imply the impossibility of a direct comparison of the results. The tubes were shaken in a head-over-head shaker for 24 h, at 80 rpm and controlled temperature (25.0 ± 0.1 °C) since, on the basis of previous studies, it was possible to attain equilibrium in these

conditions [29]. All the experiments were run in triplicate. Control experiments, consisting of the pharmaceutical solution in the absence of the adsorbent, were also run. After the defined contact time, the solutions with the suspended AC were filtered through 0.22 µm PVDF filters (Whatman) and the remaining concentration of the pharmaceutical in the aqueous solution was determined by Micellar Electrokinetic Chromatography (MEKC), as described in ESI.

All the adsorption experiments were performed in three different matrices: ultrapure water without pH adjustment (pH ~ 5.5 to 6), ultrapure water with pH adjusted to 7.6 (adjusted with 1 M sodium hydroxide and 1M hydrochloric acid) and the final effluent from an urban WWTP (pH ~ 7.6). The pH for the experiments run in ultrapure water with adjusted pH was selected according to the pH of the collected WWTP effluent. This pH was considered to be representative of urban WWTP final effluents, which would be the target application of the developed materials. The use of different aqueous media aimed at evaluating the effects of the pH and matrix complexity in the adsorption performance.

The effluent water for the adsorption experiments was collected between July and September 2018 at the outlet (after biological treatment) of a local urban WWTP (Aveiro, Portugal), designed to serve 159 700 population equivalents. The effluent was filtered through 0.45 µm membrane disc filters (Supor®, Gelman Sciences) and stored at 4 °C until use in the subsequent days.

3. Results and Discussion

The results obtained for the functionalization of the AC and their discussion are presented in two parts: the first one considers the physicochemical characterization of the AC and functionalized AC (section 3.1.), and the second part (section 3.2.) addresses the

results related with the adsorption removal of the six studied pharmaceuticals by the produced materials, in 3 different aqueous matrices.

3.1. Characterization of the synthesized materials

The physical and textural properties of the AC and functionalized AC were studied by low temperature N_2 adsorption-desorption isotherms. Figure S1 (in ESI) displays the N_2-sorption isotherms and Table 1 summarizes the textural features of the AC and functionalized AC. The presence of different micro, meso and macropores was verified. The majority of the synthesized materials present an isotherm resembling a Type Ib (IUPAC classification) [30], usually observed for microporous materials with wide micropores and possibly narrow mesopores ($\leq$ 2.5 nm). Nonetheless, the NH_2-AC presents a Type Ia isotherm (IUPAC classification) [30], typically observed in microporous materials presenting mainly narrow micropores ($\leq$ 1 nm). In all cases, some Type II (IUPAC classification) [30] character is also observed and can be associated to the presence of non-porous or macroporous fractions. All materials show a H4 hysteresis, which is often found in micro-mesoporous carbons. As can been seen in Table 1, the unmodified AC presents the highest S_{BET} of approximately 1000 $m^2 \cdot g^{-1}$ and the highest *t*-plot micropore area (S_{micro}) of above 442 $m^2 \cdot g^{-1}$. The modification of the AC with different functionalities led to a reduction of both S_{BET} and S_{micro} for all materials with exception of AC-MPTMS, where only the S_{micro} was reduced. The S_{BET} decreased in the order: AC > AC-MPTMS > AC-APTES > AC-COP > AC-NH_2. Thus, AC-NH_2 is the material with the lowest values of both S_{BET} and S_{micro}, 195 and 101 $m^2 \cdot g^{-1}$, respectively. This can be explained by the size and diffusion of the functionalization reactants into the pores of the non-functionalized AC. For example, the NH_2 group is the smallest introduced functionality, thus it is expected to be

the one that has better diffusion into the pore channels of the AC, which is confirmed by the highest reduction in the pore volume (V_p), from 0.49 $cm^3 \cdot g^{-1}$ (AC) to 0.12 $cm^3 \cdot g^{-1}$ (AC-NH_2).

Figure 2 shows a comparison of the pore size distribution (PSD) curves of AC and functionalized AC. All modifications in the AC led to a reduction of the mesopores, more pronounced in the AC-NH_2. Also, the modification of the AC promotes a slight shift to left in the pores between 1.2 and 5 nm, confirming the introduction of some functional groups into the pore channels of the parent AC. A slight reduction in the volume adsorbed into the bigger micropores (between 1.2 and 2 nm) is also observed for the functionalized AC, with exception of AC-MPTMS.

SEM micrograph images, depicted in Figure 3, show the morphological characteristics of AC, AC-NH_2 and AC-MPTMS. AC and AC-NH_2 seem to be in large aggregates of smooth surface particles almost without visible macroporosity (Figure 3a-b) while AC-MPTMS display a roughness surface particle full of macropores (Figure 3c). These characteristics are in agreement with the Type II character detected in the N_2-sorption isotherms (Table 1).

The chemical composition of the AC was verified by FTIR spectroscopy, elemental analyses and XPS. In Figure S2 (ESI) it is possible to observe the FTIR spectra of the parent AC material, where no distinguishable peaks are noticed, settling the absence of significant functionalities. The direct amine modification of the phenylene groups of the AC can be detected by the presence of two peaks at 1556 and 1197 cm^{-1} attributed to the formation of N–H and C–N bonds, respectively. The grafting of APTES and MPTMS reactants to the surface of the AC was also confirmed by FTIR (Figure S2 in ESI).The AC-COP shows peaks at 1722, 1581, 1506, 1336, 1205, 1093, 790, and 786 cm^{-1}, similar to

those observed by Mines *et al*. [18] in their functionalized AC, as for the COP contained within the matrix.

In Raman spectra (Figure S3 in ESI), one can observe that all the materials present two pronounced bands around 1300-1350 and 1600 cm^{-1} that may be attributed to D and G bands, respectively, which are typical of AC [31,32]. The D band is related to the disorder of the carbon atoms, highlighting the defects in the carbon structure. The G band is associated to the graphitic carbon, therefore, to the more ordered, symmetrical and crystalline part of the structure [31]. The materials are very similar, with the D band being more intense than the G band. Additionally, all AC present a broad band at the far wave number side (represented as the 2D or G' region, 2400 to 3250 cm^{-1}). This can be related with the presence of graphitic species. Both S–H and N–H stretching bands are difficult to be identified in the functionalized AC and should appear between 2500 and 2700 cm^{-1} and between 3100 and 3400 cm^{-1}, respectively. Both pristine AC and AC-MPTMS also show an intense band at 3450 cm^{-1}, assigned to the presence of O–H stretching modes of the phenolic or hydroxyl groups [33,34].

Table 2 shows the CHNS content of the AC and functionalized AC. The aromatic amination of the phenylene moieties of the parent AC (AC-NH_2) was successfully achieved by incorporation of 3.3% of nitrogen content. The AC-APTES and AC-MPTMS display 2.6 and 2.7% of N and S, respectively, demonstrating that the grafting reaction of APTES and MPTES functionalities with the free OH groups of the AC was effectively accomplished. These results are in agreement with those obtained by FTIR analysis (Figure S2). The AC-COP has the highest N content (11.2%) among the materials produced in this work while its S content is negligible (0.2%).

The pH_{pzc} of each of the produced materials is also depicted in Table 2. As it may be seen, the lowest pH_{pzc} is that of AC (pH_{pzc} = 3.9), while the functionalized materials displayed values between 4.9 (AC-COP) and 6.6 (AC-MPTMS).

The survey XPS spectra for AC-NH_2, AC-MPTMS, and AC are shown in Figure S4 (in ESI) along with the respective high-resolution spectra for C1s, O1s, N1s and S2p+Si2s. The results regarding the fittings and the possible bond assignments are presented in Table 3.

The overview spectra (Figure S4) show that all carbon materials present a high content in carbon followed by oxygen. In the AC-NH_2 overview spectrum it is possible to observe a peak in the N1s region, and in the AC-MPTMS spectrum a double peak in the S2p+Si2s region is observed, confirming that the functionalization of the AC succeeded. Also, in the case of AC-NH_2, a peak associated to the presence of Sn (around 490-488 eV) can be observed, possibly due to the use of $SnCl_2$ in the synthesis process.

The high-resolution spectra for C1s show that the majority of the carbon is in the graphitic form (sp^2) and as C─C and C─H (sp^3) on the edge of graphene sheets [35]. The peak at 287.2 eV is generally associated to carbon-oxygen bonds, however, some authors also ascribed this peak to C=N and C─N bonds [35,37,39,40]. The appearance or increase of this peak is expected in silylated materials (AC-MPTMS) and have been attributed to the new C─O bonds due to the unreacted alkoxy groups in organosilane [37]. The peaks at 288-289 eV can be attributed to O─C=O from carboxylic groups, anhydrides and esters [35,39] and in the case of AC-MPTMS, may be due to the presence of unreacted carboxyl.

In the N1s spectrum of AC-NH_2, the peaks at 399.6 eV and 400.3 eV are in accordance with the peak at 286.2 eV in C1s [19,37,39]. Also, the peak at 402.8 eV,

attributed to the presence of some oxidized forms of nitrogen [35,37–40,42], may be due to residual unreactive C─NO_2 species from the reduction step of the synthesis.

The O1s spectra of the different materials are very distinct from each other, indicating the presence of the same functionalities but at very different relative intensities. The peaks at 531-532 eV present a higher relative intensity for AC-MPTMS, which may be due to residual components of the synthesis.

The thermal stability of the materials was assessed by TGA up to 800 °C and both the TGA and derivative TGA (DrTGA) results are presented in Figure S5 (ESI). The first weight loss observed below 150 °C is related to desorption of physisorbed water. The parent AC presents a second decomposition at 210 °C of 3% that can be assigned to the decomposition and release of hydroxyl and carboxylic acid groups of the AC surface. The decomposition and release of other organic moieties of the AC starts around 350 °C. The modification of the phenylene moieties of the AC with the NH_2 groups was confirmed by TGA. The functional groups produced by the nitration/oxidation of the AC material and amine functionalization decompose at temperatures below 400 °C. The organic moieties' degradation and release of the AC material occurs below 615 °C (with maximum at 535 °C). The grafting modification of the AC with APTES and MPTMS leads to a slight increase in the thermal stability of the material, with the decomposition and release of amino-propyl (≈ 9%) and mercapto-propyl (≈ 6%) groups at 220 and 265 °C, respectively, followed by the decomposition of the materials that starts at approximately 390 °C. In the case of AC-COP, it presents a TGA curve that is very similar to that observed by Mines *et al.* [18] for a COP functionalized AC.

3.2. Adsorptive removal of pharmaceuticals from water

The results concerning the single adsorption of the pharmaceuticals onto AC and the functionalized materials are presented in Figure 4. Overall, among all the materials, AC-APTES is the one that presents lower adsorption percentages while AC and AC-MPTMS display the greater efficiencies for the pharmaceuticals considered. In any case, the adsorption of each pharmaceutical was very different, with PAR being the most adsorbed one, except for AC-MPTMS in ultrapure water and AC-APTES in ultrapure water and ultrapure water at pH 7.6. Contrarily, SMX was generally poorly adsorbed, except for AC-MPTMS, which furthermore showed larger SMX adsorption in the WWTP effluent than in the other matrices.

PAR presents, in all matrices, a positive net charge, which means that, in ultrapure water, π-cation interactions can be present, and in the matrices at pH 7.6, electrostatic interactions are likely to highly favor adsorption due to the negative net charge of the materials at this pH (as for the pH_{pzc}, in Table 2). Furthermore, PAR has a fluorine atom, the most electronegative halogen, which may potentiate hydrogen bonds with hydrogen bond donors such as C–H, N–H, and O–H present in the AC surfaces in the form of amines, hydroxyls and carboxyls. This may explain the differences in the adsorption of VEN, which is also positively charged in all matrices, but is consistently less adsorbed by all the AC.

Regarding CBZ and LOR, they are in the non-ionizable form ($pK_{a\mathrm{CBZ}}$ = 2.3 and 13.9; $pK_{a\mathrm{LOR}}$ = 1.3 and 11.5) in the three matrices, hence electrostatic interactions may not play a significant role in their adsorption. Some authors [45–48] have suggested that the adsorption of CBZ onto carbon materials (such as AC, graphene, carbon nanotubes) is ruled by aromatic-aromatic interactions due to the formation of π-π electron donor-acceptor

(EDA) complex between CBZ benzene ring (π-electron acceptor) and the aromatic benzene rings of AC or electron-rich carbonyl groups (π-electron donors).

SMX and PIR adsorption from ultrapure water is quite larger onto AC than onto the functionalized materials, except for AC-MPTMS. If just affected by pH related electrostatic interactions, the adsorption of these two pharmaceuticals would be expected to decrease in ultrapure water at pH 7.6 and effluent, where they are mainly in the negative form and AC also have a negative net charge. However, this is not fully verified for the adsorption of SMX onto AC and AC-MPTMS and so some specific interactions may be underneath. It has been referred that when the interactions between adsorbate and adsorbent include repulsive electrostatic forces, the increase in the ionic strength may favor adsorption [49], which could explain the relatively high adsorption of SMX onto AC-MPTMS in effluent matrix. It is important to note that the adsorption process in effluent matrix may be influenced by the presence of organic matter and also the ionic strength [49,50], which can either positively or negatively influence the adsorption depending on the adsorbent and the adsorbate. This can be clearly seen in this study, where no apparent similar pattern is observed when changing the test matrix from ultrapure water to WWTP effluent.

A principal component analysis (PCA) was carried out in order to find out possible correlations between the normalized adsorption percentages and the physicochemical properties of the studied pharmaceuticals. Results are shown in Figure S6 (ESI), which evidences that the pharmaceuticals are assembled in three groups: (i) SMX and PIR; (ii) CBZ, LOR and VEN; (iii) PAR. Adsorption onto AC-NH_2 appears to be especially affected by the pharmaceuticals hydrophobicity (log K_{ow}) and solubility (S_w) while onto AC-COP, S_w is the most relevant property. Meanwhile, for AC-MPTMS and AC-APTES, the polar

surface area (PSA) and the number of H bond acceptors (Hbond-ac) are generally the main properties influencing the pharmaceuticals adsorption.

In order to find out if there was any relation between the adsorption of pharmaceuticals and the S_{BET}, data on the adsorption percentage were normalized for the S_{BET} of the materials, as depicted in Figure S7. The normalization shows that the AC-NH_2 is the material having the largest adsorption regarding its $S_{BET.}$ Also, Figure S7 further evidences the selectivity of AC-NH_2 for the antidepressants PAR and VEN for both ultrapure water matrices (no pH adjustment and pH adjusted to 7.6) and for PAR in effluent matrix, that was intuited in Figure 4, so indicating that the S_{BET} is not the main factor influencing the adsorption of these two drugs. Some selectivity not related with S_{BET} may be also perceived for the adsorption of PAR by AC-COP (Figure S7). Aiming to schematize the influence of the AC properties, the adsorption percentage of the six pharmaceuticals onto each material was plotted *vs* its S_{BET}, S_{micro}, V_p, V_{micro}, % N, % S, and pH_{pzc}, for the three matrices (Figure S8). As it may be seen, the adsorption of each pharmaceutical from the three matrices showed a different pattern. For a more comprehensive analysis of the results, a principal component analysis (PCA) was applied to the experimental data (results are presented in Figure 5). The first and second principal components (PC1 and PC2, respectively) account for 80.5% of the variability, while the three components (PC1, PC2, and PC3) account for 93.7% of the variability, therefore, the three components were considered for the analysis.

The PCA plots (Figure 5), in particular those concerning PC1, evidence that the adsorption of the considered pharmaceuticals from the three matrices is mostly influenced by the S_{BET}, S_{micro} and V_{micro} of the AC. However, and despite AC and AC-MPTMS having similar S_{BET}, the adsorption percentages of all pharmaceuticals, except SMX, is mostly

equal or higher onto AC. Therefore, other factors may be influencing the adsorption of these pharmaceuticals in these matrices. One of those factors may be related to the pore size distribution (Figure 2). AC has a higher cumulative pore volume in the range 3-5 nm (mesopores), while AC-MPTMS has a greater prevalence of pores in the range 1-2 nm (micropores). This difference can be an important factor concerning the adsorption of pharmaceuticals, which in principle is favored by the presence of mesopores due to their large molecular size.

As illustrated by Figure 5, total pore volume (V_p) and surface functionality, namely, the amount of sulfur heteroatoms (% S) also seem to play a role in the adsorption of the studied pharmaceuticals, while the content in nitrogen (% N) looks as having little influence (Figure 5, plots PC1 *vs* PC2 and PC1 *vs* PC3). The latter is evidenced by the fact that AC-APTES, which is the material with the highest % N, visibly displays lower adsorption for all systems. In fact, even AC-NH_2, which possesses the lowest S_{BET}, shows greater adsorption percentages, in particular for positively charged pharmaceuticals (PAR and VEN), in comparison with AC-APTES. The higher adsorption of PAR and VEN onto AC-NH_2 as compared with AC-APTES, which is especially interesting since these materials are both aminated, cannot be explained by the textural properties. Therefore, it may be related to differences in the surface chemistry of the materials. AC-NH_2 has aromatic amino groups at the surface, while AC-APTES has propyl amino groups. Additionally, AC-NH_2 presents tin oxide (SnO_2) nanoparticles that can influence the interaction with PAR and VEN (Figure S4a). Thus, this improvement in the adsorption properties of the AC-NH_2 can be also related to acid–base and electrostatic interactions of PAR and VEN with the Lewis acid sites of SnO_2 [51,52].

Apart from the previously commented, another materials' property included in the PCA was pH_{pzc}. pH is known to have an important role in the adsorption mechanism as it affects the protonation or deprotonation of the adsorbates and the surface charge of the AC [53]. The introduction of different functionalities onto the AC surface resulted in materials with different pH_{pzc} (between 3.9 and 6.6, Table 2). Still, in each matrix, all the AC are in the same protonation state. Thereupon, as for the PCA results (Figure 5), pH_{pzc} appears to have no relevant influence in the adsorption of the studied pharmaceuticals.

In view of the above results, it may be stated that, globally, the parent AC followed by AC-MPTMS were the materials providing the best adsorptive performance for the considered pharmaceuticals and matrices. This must be related with the reduction in S_{BET} that, except for AC-MPTMS, resulted from functionalization. Still, it was here observed that some functionalized AC shown remarkable properties and/or a distinct behavior that may be useful for specific applications. Considering that this is a pioneer work on the functionalization of waste derived AC, the obtained results are the basis for a novel research line. In order to further elucidate the mechanistic aspects that rule the adsorption process, in particular for the materials that presented the best removal percentages, kinetic, equilibrium and thermodynamic studies will be the focus of future works. Also, it would be relevant to decrease the impact of functionalization on the S_{BET} to allow for and improve the adsorption of a wider range of pharmaceuticals. This may be especially relevant in the case of antibiotics, which are generally poorly adsorbed and whose presence in the aquatic environment is related to antibiotic resistance. Additional applications of the functionalized materials, namely in the adsorptive removal of other pollutants, are also to be studied.

4. Conclusions

The functionalization of a paper mill sludge-based AC was successfully achieved considering the addition of the specific functional groups onto the AC: amine groups (AC-NH_2 and AC-APTES), sulfonic groups (AC-MPTMS), and a covalent organic polymer (AC-COP). Comparatively with the parent AC, this addition resulted in the reduction of both S_{BET} and S_{micro} for all materials with exception of AC-MPTMS, for which just S_{micro} decreased. The application of the functionalized AC in the removal of the six pharmaceuticals considered in this study (CBZ, LOR, SMX, PIR, PAR and VEN) from ultrapure water, ultrapure water at pH 7.6 and effluent from a WWTP revealed that the adsorption of each pharmaceutical in each matrix showed distinct patterns, with the non-funcionalized AC mostly displaying the best performance. Textural parameters, namely S_{BET}, S_{micro} and V_{micro} had the greatest influence in the adsorption of these pharmaceuticals, with V_p and % S also playing a role and % N having little repercussion. On the other hand, according to their pH_{pzc}, the produced AC were all at the same protonation state in each matrix, so pH_{pzc} was not a key property for the adsorption of the pharmaceuticals.

Regarding the impacts of functionalization for the target application, it may be said that grafting the organic polymer is a time-consuming process and AC-COP did not present any enhancement in the adsorption of pharmaceuticals. When comparing AC-APTES with AC-NH_2, despite the former having highest S_{BET}, it showed a poorer performance than AC-NH_2. On the other hand, AC-NH_2 showed some specificity for the antidepressants PAR and VEN, which may be advantageous. Regarding AC-MPTMS, it was the functionalized material providing the best global performance, which was almost comparable to that of the parent AC. Still, the remarkable affinity of AC-MPTMS for SMX in wastewater may be a relevant feature for specific applications. Overall, despite the decrease of the adsorption

properties of the AC after functionalization, the selectivity of the AC modified with MPTMS and aromatic amino groups increase, which is advantageous for the selective removal of pharmaceuticals. This was a pioneering work on the functionalization of waste derived AC with novel results on the properties and application of the functionalized materials that opens a new research line in this field.

Associated content

Electronic Supplementary information (ESI) available.

Notes

The authors declare no competing financial interest.

Acknowledgments

This work is a contribution to the projects RemPharm and WasteMAC (PTDC/AAG-TEC/1762/2014 and POCI-01-0145-FEDER-028598, respectively) funded by FCT – Fundação para a Ciência e a Tecnologia, I.P., through national funds, and the co-funding by the FEDER, within the PT2020 Partnership Agreement and Compete 2020. Thanks are also due for the financial support to CESAM (UID/AMB/50017/2019), to FCT/MEC through national funds, and the co-funding by the FEDER, within the PT2020 Partnership Agreement and Compete 2020. This work was also developed within the scope of the project CICECO-Aveiro Institute of Materials, FCT Ref. UID/CTM/50011/2019, financed by national funds through the FCT/MCTES. GJ thanks FCT for her PhD grant (SFRH/BD/138388/2018); MO and PF are thankful to FCT for the Investigator Program (IF/00314/2015 and IF/00300/2015, respectively) and VC is thankful to FCT for Scientific

Employment Stimulus (CEECIND/00007/2017). Milton Fontes and workers of Aveiro's WWTP (Águas do Centro Litoral) are gratefully acknowledged for assistance on the effluent sampling campaigns.

References

[1] E.N. Evgenidou, I.K. Konstantinou, D.A. Lambropoulou, Occurrence and removal of transformation products of PPCPs and illicit drugs in wastewaters: A review, Sci. Total Environ. 505 (2015) 905–926. doi:10.1016/j.scitotenv.2014.10.021.

[2] Y. Yang, Y.S. Ok, K.H. Kim, E.E. Kwon, Y.F. Tsang, Occurrences and removal of pharmaceuticals and personal care products (PPCPs) in drinking water and water/sewage treatment plants: A review, Sci. Total Environ. 596–597 (2017) 303–320. doi:10.1016/j.scitotenv.2017.04.102.

[3] V. Calisto, V.I. Esteves, Psychiatric pharmaceuticals in the environment, Chemosphere. 77 (2009) 1257–1274. doi:10.1016/j.chemosphere.2009.09.021.

[4] A.J. Ebele, M. Abou-Elwafa Abdallah, S. Harrad, Pharmaceuticals and personal care products (PPCPs) in the freshwater aquatic environment, Emerg. Contam. 3 (2017) 1–16. doi:10.1016/j.emcon.2016.12.004.

[5] P. Sehonova, Z. Svobodova, P. Dolezelova, P. Vosmerova, C. Faggio, Effects of waterborne antidepressants on non-target animals living in the aquatic environment: A review, Sci. Total Environ. 631–632 (2018) 789–794. doi:10.1016/j.scitotenv.2018.03.076.

[6] European Parliament, Directive 2013/39/EU of the European Parliament and of the Council of 12 August 2013 amending Directives 2000/60/EC and 2008/105/EC as regards priority substances in the field of water policy, Official Journal of the

European Union (2013).

[7] C.P. Silva, G. Jaria, M. Otero, V.I. Esteves, V. Calisto, Waste-based alternative adsorbents for the remediation of pharmaceutical contaminated waters: Has a step forward already been taken?, Bioresour. Technol. 250 (2018) 888–901. doi:10.1016/j.biortech.2017.11.102.

[8] J.R. De Andrade, M.F. Oliveira, M.G.C. Da Silva, M.G.A. Vieira, Adsorption of pharmaceuticals from water and wastewater using non conventional low-cost materials: A Review, Ind. Eng. Chem. Res. 57 (2018) 3103–3127. doi:10.1021/acs.iecr.7b05137.

[9] L. Paredes, E. Fernandez-Fontaina, J.M. Lema, F. Omil, M. Carballa, Understanding the fate of organic micropollutants in sand and granular activated carbon biofiltration systems, Sci. Total Environ. 551–552 (2016) 640–648. doi:10.1016/j.scitotenv.2016.02.008.

[10] V. Rakić, V. Rac, M. Krmar, O. Otman, A. Auroux, The adsorption of pharmaceutically active compounds from aqueous solutions onto activated carbons, J. Hazard. Mater. 282 (2015) 141–149. doi:10.1016/j.jhazmat.2014.04.062.

[11] G. Jaria, C.P. Silva, J.A.B.P. Oliveira, S.M. Santos, M.V. Gil, M. Otero, V. Calisto, V.I. Esteves, Production of highly efficient activated carbons from industrial wastes for the removal of pharmaceuticals from water - A full factorial design, J. Hazard. Mater. 370 (2019) 212-218. doi:10.1016/j.jhazmat.2018.02.053.

[12] H. Guedidi, L. Reinert, Y. Soneda, N. Bellakhal, L. Duclaux, Adsorption of ibuprofen from aqueous solution on chemically surface-modified activated carbon cloths, Arab. J. Chem. 10 (2017) S3584–S3594. doi:10.1016/j.arabjc.2014.03.007.

[13] C.Y. Yin, M.K. Aroua, W.M.A.W. Daud, Review of modifications of activated

carbon for enhancing contaminant uptakes from aqueous solutions, Sep. Purif. Technol. 52 (2007) 403–415. doi:10.1016/j.seppur.2006.06.009.

[14] G.G. Stavropoulos, P. Samaras, G.P. Sakellaropoulos, Effect of activated carbons modification on porosity, surface structure and phenol adsorption, J. Hazard. Mater. 151 (2008) 414–421. doi:10.1016/j.jhazmat.2007.06.005.

[15] J. Rivera-Utrilla, M. Sánchez-Polo, V. Gómez-Serrano, P.M. Álvarez, M.C.M. Alvim-Ferraz, J.M. Dias, Activated carbon modifications to enhance its water treatment applications. An overview, J. Hazard. Mater. 187 (2011) 1–23. doi:10.1016/j.jhazmat.2011.01.033.

[16] A. Bhatnagar, W. Hogland, M. Marques, M. Sillanpää, An overview of the modification methods of activated carbon for its water treatment applications, Chem. Eng. J. 219 (2013) 499–511. doi:10.1016/j.cej.2012.12.038.

[17] B.N. Bhadra, P.W. Seo, S.H. Jhung, Adsorption of diclofenac sodium from water using oxidized activated carbon, Chem. Eng. J. 301 (2016) 27–34. doi:10.1016/j.cej.2016.04.143.

[18] P.D. Mines, D. Thirion, B. Uthuppu, Y. Hwang, M.H. Jakobsen, H.R. Andersen, C.T. Yavuz, Covalent organic polymer functionalization of activated carbon surfaces through acyl chloride for environmental clean-up, Chem. Eng. J. 309 (2017) 766–771. doi:10.1016/j.cej.2016.10.085.

[19] J.L. Figueiredo, Functionalization of porous carbons for catalytic applications, J. Mater. Chem. A. 1 (2013) 9351–9364. doi:10.1039/c3ta10876g.

[20] V.Z. Radkevich, T.L. Senko, K. Wilson, L.M. Grishenko, A.N. Zaderko, V.Y. Diyuk, The influence of surface functionalization of activated carbon on palladium dispersion and catalytic activity in hydrogen oxidation, Appl. Catal. A Gen. 335

(2008) 241–251. doi:10.1016/j.apcata.2007.11.029.

[21] E. Lebègue, T. Brousse, J. Gaubicher, C. Cougnon, Chemical functionalization of activated carbon through radical and diradical intermediates, Electrochem. Commun. 34 (2013) 14–17. doi:10.1016/j.elecom.2013.05.014.

[22] G. Pognon, T. Brousse, D. Bélanger, Effect of molecular grafting on the pore size distribution and the double layer capacitance of activated carbon for electrochemical double layer capacitors, Carbon, 49 (2011) 1340–1348. doi:10.1016/j.carbon.2010.11.055.

[23] E. Lebègue, L. Madec, T. Brousse, J. Gaubicher, E. Levillain, C. Cougnon, Modification of activated carbons based on diazonium ions in situ produced from aminobenzene organic acid without addition of other acid, J. Mater. Chem. 21 (2011) 12221–12223. doi:10.1039/c1jm11538c.

[24] E. Lebègue, T. Brousse, J. Gaubicher, C. Cougnon, Spontaneous arylation of activated carbon from aminobenzene organic acids as source of diazonium ions in mild conditions, Electrochim. Acta. 88 (2013) 680–687. doi:10.1016/j.electacta.2012.10.132.

[25] M.A.O. Lourenço, C. Siquet, J. Santos, M. Jorge, J.R.B. Gomes, P. Ferreira, Insights into CO_2 and CH_4 adsorption by pristine and aromatic amine-modified periodic mesoporous phenylene-silicas, J. Phys. Chem. C. 120 (2016) 14236–14245. doi:10.1021/acs.jpcc.6b04605.

[26] M.A.O. Lourenço, P. Figueira, E. Pereira, J.R.B. Gomes, C.B. Lopes, P. Ferreira, Simple, mono and bifunctional periodic mesoporous organosilicas for removal of priority hazardous substances from water: The case of mercury(II), Chem. Eng. J. 322 (2017) 263–274. doi:10.1016/j.cej.2017.04.005.

[27] O. Inagaki, S.; Guan, S.; Ohsuna, T.; Terasaki, An ordered mesoporous organosilica hybrid material with a crystal-like wall structure, Nature. (2002) 304–307.

[28] M. Ohashi, M.P. Kapoor, S. Inagaki, Chemical modification of crystal-like mesoporous phenylene-silica with amino group, Chem. Commun. (2008) 841–843. doi:10.1039/b716141g.

[29] C.P. Silva, G. Jaria, M. Otero, V.I. Esteves, V. Calisto, Adsorption of pharmaceuticals from biologically treated municipal wastewater using paper mill sludge-based activated carbon, Environ. Sci. Pollut. Res. 26 (2019) 13173–13184. doi:10.1007/s11356-019-04823-w.

[30] K.S.W. Sing, D.H. Everett, R.A.W. Haul, L. Moscou, R.A. Pierotti, J. Rouquerol, T. Siemieniewska, Reporting physisorption data for gas/solid systems with special reference to the determination of surface area and porosity., Pure Appl. Chem. 57 (1985) 603–619.

[31] L. Alcaraz, A. L Opez Fernández, I. Garc Ia-D Iaz, F. Lix, A.L. Opez, Preparation and characterization of activated carbons from winemaking wastes and their adsorption of methylene blue, Adsorpt. Sci. Technol. 36 (2018) 1331–1351. doi:10.1177/0263617418770295.

[32] K. Glonek, A. Wróblewska, E. Makuch, B. Ulejczyk, K. Krawczyk, R.J. Wróbel, Z.C. Koren, B. Michalkiewicz, Oxidation of limonene using activated carbon modified in dielectric barrier discharge plasma, Appl. Surf. Sci. 420 (2017) 873–881. doi:10.1016/J.APSUSC.2017.05.136.

[33] F. Adar, Introduction to interpretation of raman spectra using database searching and functional group detection and identification, 2016.

[34] Peter Larkin, Infrared and raman spectroscopy principles and spectral interpretation,

1st ed., Elsevier, USA, 2011.

[35] I. Velo-Gala, J.J. López-Peñalver, M. Sánchez-Polo, J. Rivera-Utrilla, Surface modifications of activated carbon by gamma irradiation, Carbon N. Y. 67 (2014) 236–249. doi:10.1016/j.carbon.2013.09.087.

[36] X. Ma, H. Yang, L. Yu, Y. Chen, Y. Li, Preparation, surface and pore structure of high surface area activated carbon fibers from bamboo by steam activation, Materials 7 (2014) 4431–4441. doi:10.3390/ma7064431.

[37] H. Gaspar, C. Pereira, S.L.H. Rebelo, M.F.R. Pereira, J.L. Figueiredo, C. Freire, Understanding the silylation reaction of multi-walled carbon nanotubes, Carbon 49 (2011) 3441–3453. doi:10.1016/j.carbon.2011.04.041.

[38] J.L. Figueiredo, M.F.R. Pereira, The role of surface chemistry in catalysis with carbons, Catal. Today. 150 (2010) 2–7. doi:10.1016/j.cattod.2009.04.010.

[39] M.S. Lee, M. Park, H.Y. Kim, S.J. Park, Effects of microporosity and surface chemistry on separation performances of N-containing pitch-based activated carbons for CO_2/N_2 binary mixture, Sci. Rep. 6 (2016) 1–11. doi:10.1038/srep23224.

[40] T. Susi, T. Pichler, P. Ayala, X-ray photoelectron spectroscopy of graphitic carbon nanomaterials doped with heteroatoms, Beilstein J. Nanotechnol. 6 (2015) 177–192. doi:10.3762/bjnano.6.17.

[41] M. Zhu, C.J. Weber, Y. Yang, M. Konuma, U. Starke, K. Kern, A.M. Bittner, Chemical and electrochemical ageing of carbon materials used in supercapacitor electrodes, Carbon 46 (2008) 1829–1840. doi:10.1016/j.carbon.2008.07.025.

[42] T. Wei, Q. Zhang, X. Wei, Y. Gao, H. Li, A Facile and low-cost route to heteroatom doped porous carbon derived from broussonetia papyrifera bark with excellent supercapacitance and CO_2 capture performance, Sci. Rep. 6 (2016) 2–10.

doi:10.1038/srep22646.

[43] B. Martín-García, A. Polovitsyn, M. Prato, I. Moreels, Efficient charge transfer in solution-processed PbS quantum dot-reduced graphene oxide hybrid materials, J. Mater. Chem. C. 3 (2015) 7088–7095. doi:10.1039/c5tc01137j.

[44] A.D. Roberts, X. Li, H. Zhang, Hierarchically porous sulfur-containing activated carbon monoliths via ice-templating and one-step pyrolysis, Carbon 95 (2015) 268–278. doi:10.1016/j.carbon.2015.08.004.

[45] N. Cai, P. Larese-Casanova, Sorption of carbamazepine by commercial graphene oxides: A comparative study with granular activated carbon and multiwalled carbon nanotubes, J. Colloid Interface Sci. 426 (2014) 152–161. doi:10.1016/j.jcis.2014.03.038.

[46] M. Baghdadi, E. Ghaffari, B. Aminzadeh, Removal of carbamazepine from municipal wastewater effluent using optimally synthesized magnetic activated carbon: Adsorption and sedimentation kinetic studies, J. Environ. Chem. Eng. 4 (2016) 3309–3321. doi:10.1016/j.jece.2016.06.034.

[47] D. Chen, S. Xie, C. Chen, H. Quan, L. Hua, X. Luo, L. Guo, Activated biochar derived from pomelo peel as a high-capacity sorbent for removal of carbamazepine from aqueous solution, RSC Adv. 7 (2017) 54960–54979. doi:10.1039/c7ra10805b.

[48] C.H.M. Hofman-Caris, P.S. Bäuerlein, W.G. Siegers, J. Ziaie, H.H. Tolkamp, P. De Voogt, Affinity adsorption for the removal of organic micropollutants in drinking water sources; Proof of principle, Water Sci. Technol. Water Supply. 15 (2015) 1207–1219. doi:10.2166/ws.2015.084.

[49] F. Reguyal, A.K. Sarmah, Adsorption of sulfamethoxazole by magnetic biochar: Effects of pH, ionic strength, natural organic matter and 17α-ethinylestradiol, Sci.

Total Environ. 628–629 (2018) 722–730. doi:10.1016/j.scitotenv.2018.01.323.

[50] H.A. Arafat, M. Franz, N.G. Pinto, Effect of salt on the mechanism of adsorption of aromatics on activated carbon, Langmuir. 15 (1999) 5997–6003. doi:10.1021/la9813331.

[51] Vidal, C. B., A.B. dos Santos, T.J. do Nascimento, R. F. Bandosz, Reactive adsorption of pharmaceuticals on tin oxide pillared montmorillonite: Effect of visible light exposure., Chem. Eng. J. 259 (2015) 865–875.

[52] A. Shamsizadeh, M. Ghaedi, A. Ansari, S. Azizian, M.K. Purkait, Tin oxide nanoparticle loaded on activated carbon as new adsorbent for efficient removal of malachite green-oxalate: Non-linear kinetics and isotherm study., J. Mol. Liq. 195 (2014) 212–218.

[53] J.Y. Song, B.N. Bhadra, S.H. Jhung, Contribution of H-bond in adsorptive removal of pharmaceutical and personal care products from water using oxidized activated carbon, Microporous Mesoporous Mater. 243 (2017) 221–228. doi:10.1016/j.micromeso.2017.02.024.

Declaration of interests

☒ The authors declare that they have no known competing financial interests or personal relationships that could have appeared to influence the work reported in this paper.

☐The authors declare the following financial interests/personal relationships which may be considered as potential competing interests:

The corresponding author, on behalf of all authors,

Figure captions

Figure 1. Schematic representation of the functionalization procedures: A- Direct amination; B – Organosilane grafting with APTES; C – Organosilane grafting with MPTMS; and D – functionalization with an organic polymer (COP-19, based on Mines *et al*. [18]).

Figure 2. Pore size distribution of AC and functionalized AC. Pore width was obtained from the non-linear density functional theory (NLDFT).

Figure 3. SEM images of crushed samples of a) AC, b) AC-NH_2, and c) AC-MPTMS.

Figure 4. Adsorption of the six studied pharmaceuticals (CBZ, LOR, SMX, PIR, PAR and VEN) in different matrices (ultrapure water, ultrapure water at pH 7.6 and WWTP effluent) onto the AC and the functionalized AC. Error bars correspond to standard deviations (n = 3).

Figure 5. PCA plots for the principal components PC1, PC2 and PC3. Ultrapure water, ultrapure water with pH adjusted to 7.6 and WWTP effluent are represented by the colored solid lines, dash lines and dotted lines, respectively. Black lines correspond to the physicochemical characteristics considered in this analysis.

Table 1. Textural properties of AC and functionalized AC.

Sample	S_{BET} / $m^2 \cdot g^{-1}$	S_{micro} [a] / $m^2 \cdot g^{-1}$	V_P [a] / $cm^3 \cdot g^{-1a}$	V_{micro} [a] / $cm^3 \cdot g^{-1a}$	Isotherm type (hysteresis)
AC	994	442	0.49	0.19	Ib + II (H4)
AC-NH_2	195	101	0.12	0.04	Ia + II (H3)
AC-APTES	650	207	0.43	0.09	Ib + II (H4)
AC-MPTMS	993	379	0.56	0.17	Ib + II (H4)
AC-COP	410	98	0.34	0.06	Ib + II (H4+H3)

[a] S_{micro} (microporous area) and V_{micro} (micropore volume) values were determined by the *t*-plot method. [b]V_p corresponds to the Barret-Joyner-Halenda (BJH) adsorption cumulative pore volume applying the Kruk-Jaroniec-Sayari correction.

Table 2. Elemental analyses and point of zero charge (pH_{pzc}) of AC and functionalized AC.

Sample	% C	% H	% N	% S	H/C	pH_{pzc}
AC	58.2	1.1	0.6	0.3	0.019	3.9
AC-NH_2	50.1	3.2	3.3	0.5	0.064	5.2
AC-APTES	54.1	2.2	2.6	0.6	0.040	6.6
AC-MPTMS	55.7	1.0	0.4	2.7	0.018	5.2
AC-COP	51.3	2.9	11.2	0.2	0.057	4.9

Table 3. X-ray photoelectron spectroscopy (XPS) results for AC, AC-NH_2 and AC-MPTMS.

		AC-NH_2	**AC-MPTMS**	**AC [29]**	
	Peak	**Binding Energy (eV)**	**Binding Energy (eV)**	**Binding Energy (eV)**	**Possible bond assignment**
C 1s	**1**	284.9	284.3	284.4	Graphitic C (sp^2) [35]
	2		285.3	285.3	C-C on the edge of graphene sheets (sp3) C-H [35]
		286.2			Single bond C-O (phenolic or hydroxyl groups) [35,36]
	3		286.2	286.1	C─C bonds from the organosilane alkyl chain [37] (for AC-MPTMS)
					C─N bonds of aliphatic amines groups or due to the incomplete reduction of C─NO_2 in the synthesis step [37,38] (in particular for AC-NH_2)
		287.2			Carbon-oxygen bonds; C=N and C─N bonds [35,37,39,40]
	4		287.2		C─O bonds due to the unreacted alkoxy groups in organosilane [37] (for AC_MPTMS)
		288.7			O─C=O from carboxylic groups, anhydrides and

	5		288.5	289.2	esters [35,39]
		290.0			π- π* transitions in C [35]
	6		290.4	290.5	
		291.7			Plasmon band in C [41]
O 1s	**1**	531.6	532.0	531.1	Carbonyl (–C=O) oxygen atoms in lactones, anhydrides and oxygen atoms in hydroxyl groups [19,35]
	2	533.6	533.5	532.6	–C–O–C– in ether and phenol groups [37]
	3			533.9	Oxygen in carboxylic groups (–COOH or –COOR) [35]
		535.8	536.1		Chemisorbed water or oxygen [35]
	4			536	
N 1s	**1**	399.6		397.7	Nitrogen from amine, imine or amide groups (─NH_2, C=N, N─C=O) [19,37,39]
	2	400.3		399.6	Pyridonic or pyrrolic nitrogen (N5) [35,37–40,42]
	3	401.6		401.5	Quaternary nitrogen (N-Q) [35,37–40,42]
	4	402.9		402.9	Nitrogen oxides or nitrates (N-X) [35,37–40,42]
Si2s+S2p	**1**		153.3		Silanes [43]
	2		154.0		
	3		163.1		Thiol moieties (–SH) [37,43]
	4		164.1		Sulfur-carbon (S–C) bonds [37,43]
	5		168.2		Sulfoxide groups [44]

Graphical abstract

Highlights

1. An alternative activated carbon (AC) was functionalized with N and S groups
2. The functionalized ACs were tested for the adsorption of 6 pharmaceuticals
3. Adsorption tests were done in water, water with adjusted pH 7.6 and wastewater
4. Textural parameters were the most influencing factors in pharmaceuticals adsorption
5. The functionalized ACs showed distinct behaviour for the different pharmaceuticals

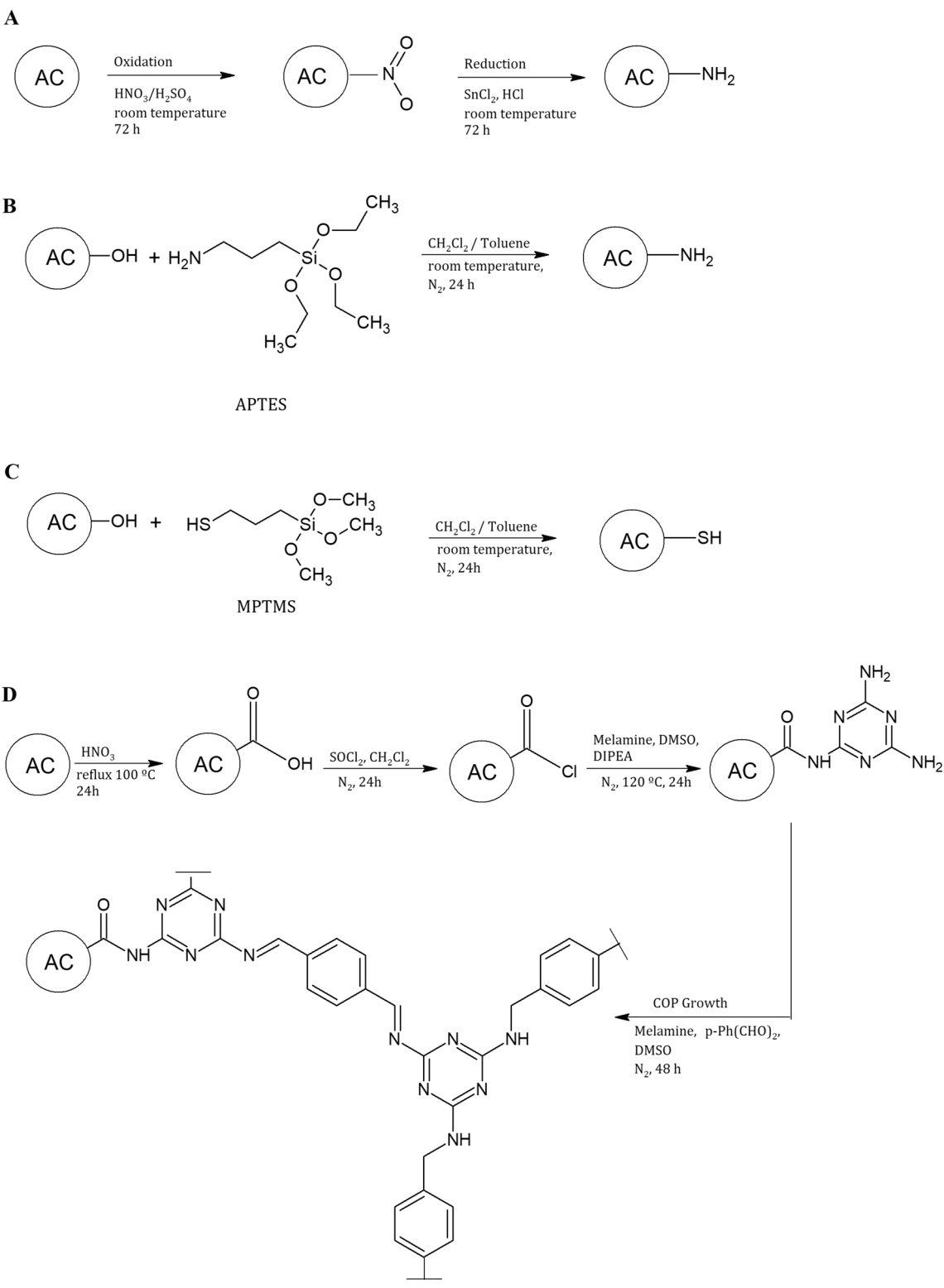
A
AC
Oxidation
HNO3/H2SO4
room temperature
72 h
AC
N
O
O
Reduction
SnCl2, HCl
room temperature
72 h
AC
NH2
B
AC
OH + H2N
Si
O
CH3
CH2Cl2 / Toluene
room temperature,
N2, 24 h
AC
NH2
APTES
C
AC
OH +
HS
Si
O
CH3
CH2Cl2 / Toluene
room temperature,
N2, 24h
AC
SH
MPTMS
D
AC
HNO3
reflux 100 ºC
24h
AC
OH
SOCl2, CH2Cl2
N2, 24h
AC
Cl
Melamine, DMSO,
DIPEA
N2, 120 ºC, 24h
AC
NH2
NH
NH2
AC
NH
NH
COP Growth
Melamine, p-Ph(CHO)2,
DMSO
N2, 48 h

Figure 1

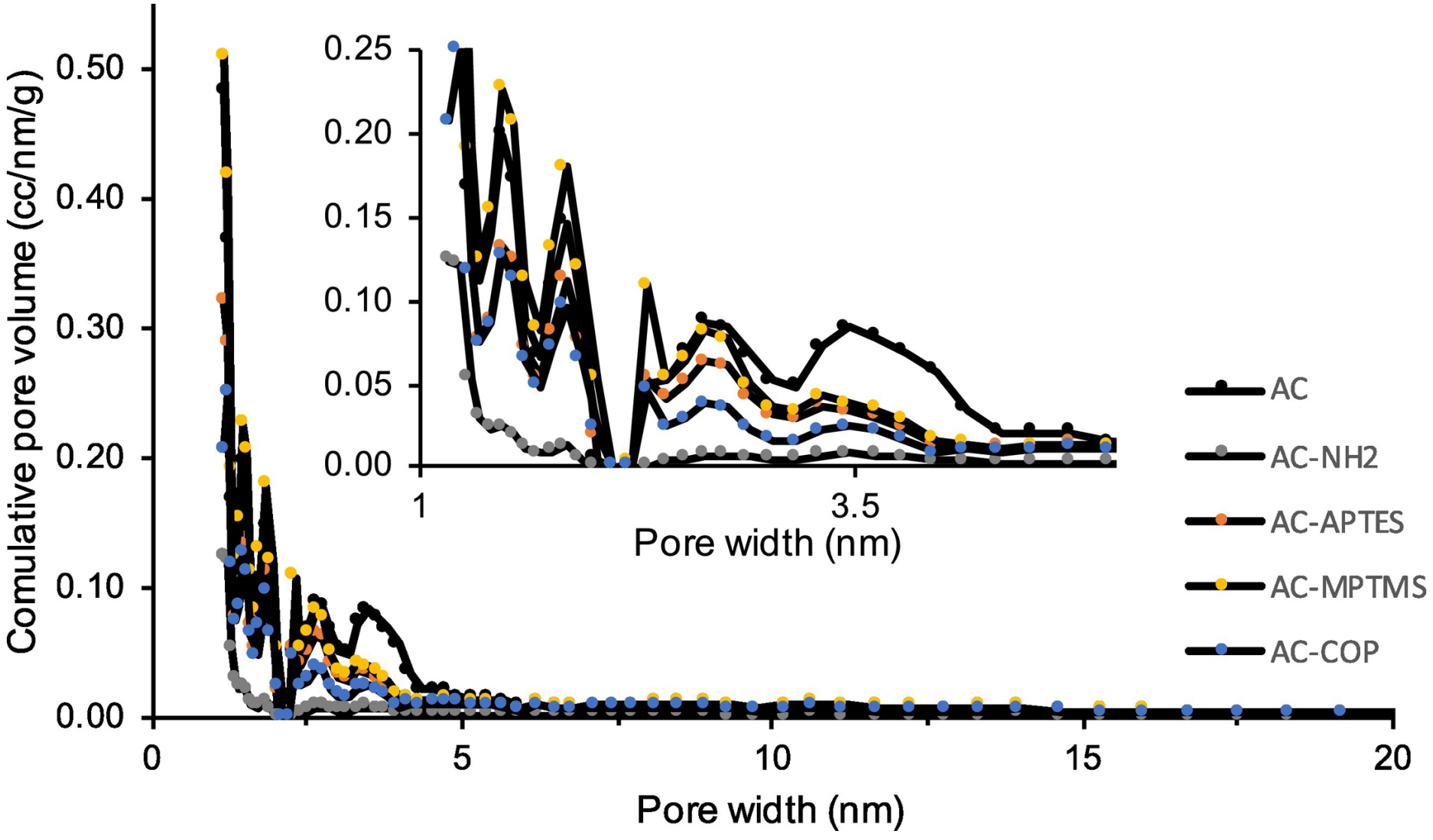
Comulative pore volume (cc/nm/g)
0.50
0.40
0.30
0.20
0.10
0.00
0
5
10
15
20
Pore width (nm)
0.25
0.20
0.15
0.10
0.05
0.00
1
3.5
Pore width (nm)
AC
AC-NH2
AC-APTES
AC-MPTMS
AC-COP

Figure 2

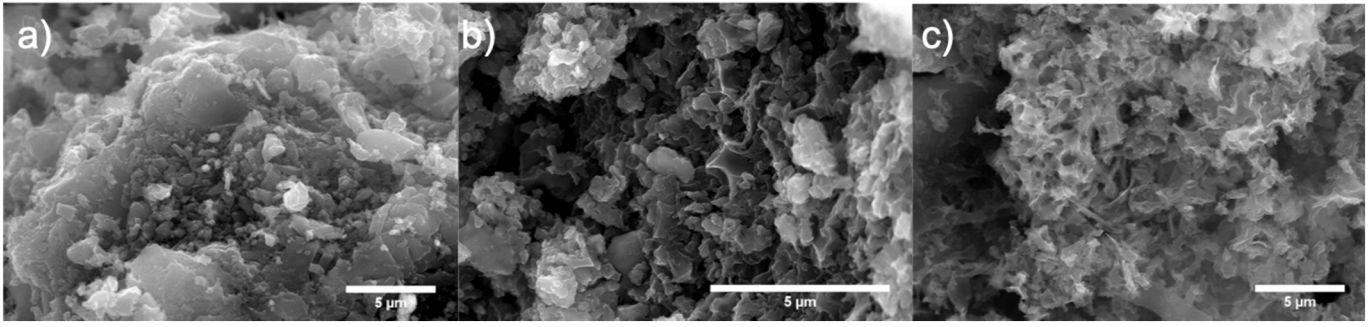

Figure 3

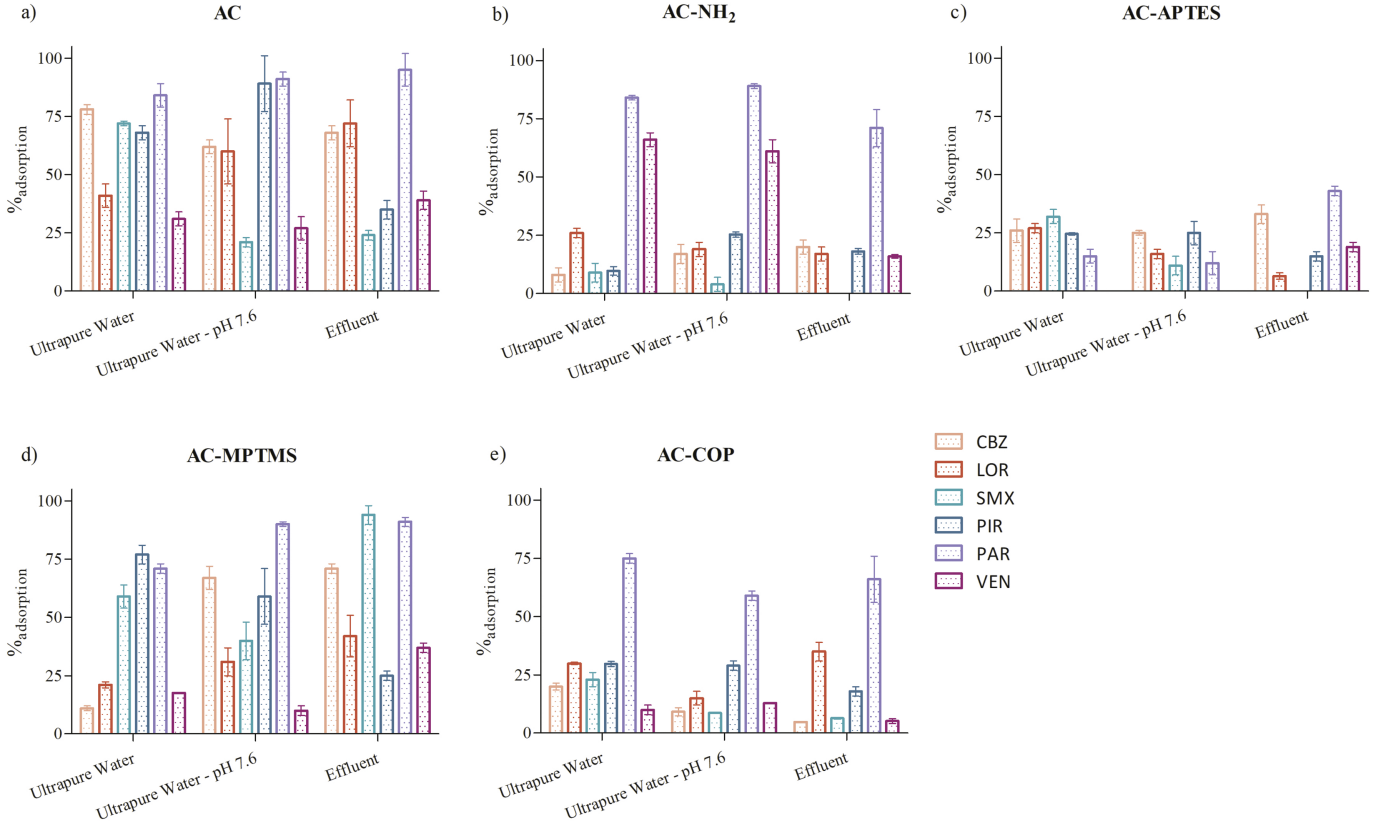
a)
AC
b)
AC-NH2
c)
AC-APTES
d)
AC-MPTMS
e)
AC-COP
%adsorption
100
75
50
25
0
Ultrapure Water
Ultrapure Water - pH 7.6
Effluent
CBZ
LOR
SMX
PIR
PAR
VEN

Figure 4

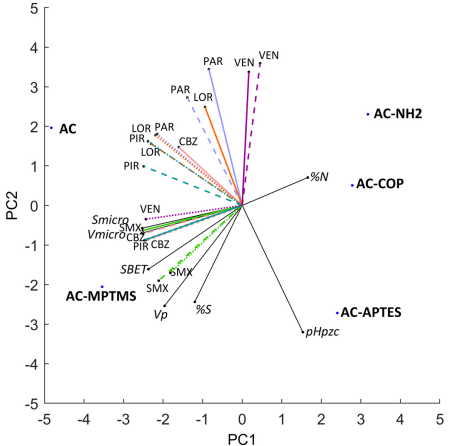
PC1
PC2
AC
AC-NH2
AC-COP
AC-APTES
AC-MPTMS
PAR
VEN
LOR
PIR
CBZ
SMX
%N
%S
pHpzc
Smicro
Vmicro
SBET
Vp

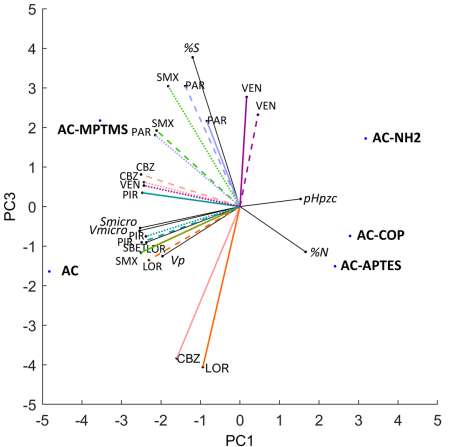
PC1
PC3
AC
AC-NH2
AC-COP
AC-APTES
AC-MPTMS
%S
SMX
PAR
VEN
CBZ
LOR
PIR
pHpzc
%N
Smicro
Vmicro
SBET
Vp

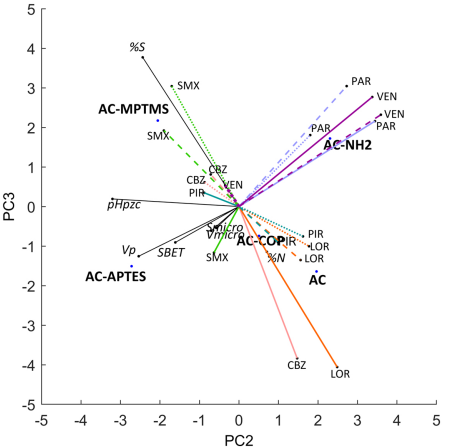
PC2
PC3
AC
AC-NH2
AC-COP
AC-APTES
AC-MPTMS
%S
SMX
PAR
VEN
CBZ
LOR
PIR
pHpzc
%N
Smicro
Vmicro
SBET
Vp

Figure 5